Sorption studies of europium on cerium phosphate using Box-Behnken design

Süleyman İNAN[*]
Institute of Nuclear Sciences, Ege University, İzmir, Turkey

Abstract: Amorphous cerium phosphate was prepared and characterized. Three-level Box-Behnken design (BBD) was employed to analyze the effect of process variables such as initial pH (2–6), contact time (60–180 min), and sorbent amount (0.05–0.15 g) on the sorption capacity of europium. Analysis of variance (ANOVA) revealed that the main effect of initial pH and sorbent amount has a substantial impact on the sorption of Eu(III). Probability F-value (F = 3 × 10^{-3}) and correlation coefficient (R^2 = 0.97) point out that the model is in good accordance with experimental data. The maximum sorption capacity of Eu(III) was found to be 42.14 mg g^{-1} at initial pH 6, contact time of 180 min, and a sorbent amount of 0.05 g. Sorption isotherm data was well explained by the Langmuir model and monolayer Eu(III) sorption capacity was obtained as 30.40 mg g^{-1}. Kinetic data were well described by the pseudo-second-order model. Thermodynamic data suggested that the process is endothermic and spontaneous.

Key words: Sorption, europium, cerium phosphate, Box-Behnken, separation

1. Introduction

Rare earth elements (REEs) are a group of metals consisting of 15 lanthanide elements including yttrium and scandium. Owing to their superior physical and chemical properties, they are significant for several progressive technologies [1]. Among them, europium (Eu) is an active metal; a trace amount of europium may greatly enhance the properties of metals [2]. Europium is used in light-emitting diodes (LEDs), LCDs, and fluorescent lamps. Because of the growing demand for LEDs and LCDs, it is becoming a more vital element for the electronic industry [3]. Europium is also used in nuclear reactor control rods because of its neutron absorption effectiveness[1]. The demand for europium supply has been increasing every day. However, europium sources are not equally distributed on Earth, and the production of europium in the world is mostly in China [3]. Therefore, recovery of europium and other REEs from alternative sources such as electronic waste and wastewater has become an important issue.

On the other hand, during the operation of nuclear power plants radioactive europium ($^{152+154}$Eu) is produced in low-level radioactive waste solutions together with ^{137}Cs. Because of its long half-life, separation of europium from radioactive wastes before discharge is very significant [4]. Recovery and removal of europium from a different type of waste solutions are of great importance not only from the point of their limited resource availability but also for the mitigation of their quantity for disposal as radioactive wastes.

---

[*]Correspondence: inansuleyman@gmail.com

[1]Peterson J, Macdonell M, Haroun L, Monette F, Hildebrand RD et al. (2007). "Europium" in Radiological and Chemical Fact Sheets to Support Health Risk Analyses for Contaminated Areas [online]. Website https://www.remm.nlm.gov/ANL_ContaminantFactSheets_All_070418.pdf [accessed 01 November 2019].

Sorption is one of the most promising techniques due to its advantages of high efficiency, low operation temperature, and high selectivity. Various types of materials such as goethite [5], aluminum silicate [6], aluminum oxide [4], functionalized magnetic chitosan [7], montmorillonites [8], manganese oxides [9], biomass [10] and algae [3] were used as sorbents/ion exchangers to remove and separate europium from radioactive waste and aqueous streams.

Insoluble salts of tetravalent metals are composed of tetravalent metal salts and anions like phosphate, molybdate, antimonate, etc. Inorganic ion exchangers/sorbents consisted of tetravalent metal acid salts are highly stable in strong acids, oxidizing solutions, and ionizing radiations. They show selectivity for certain metal ions. In particular, they are attractive for applications where organic resins cannot be used because of their degradability [11]. Cerium(IV) tungstate [12], titanium(IV) phosphates [13,14], poly-acrylamide based cerium(IV) phosphate [15], zirconium(IV) molybdate [16] have been utilized for the sorption of europium ions.

Cerium phosphate compounds have been prepared [17–19] and used for the separation of some radionuclides [15,20] from hazardous waste solutions. But so far, there is no study reported in the literature focused on the sorption behavior of neat cerium phosphate towards europium.

In the present study, amorphous cerium phosphate was prepared, characterized, and used as a sorbent for the separation of Eu(III) ions from aqueous solution. Response surface methodology (RSM) was utilized to analyze the effect of initial pH, contact time, and sorbent amount on sorption capacity. For this aim, Box-Behnken Design (BBD) with 3 variables was employed. Equilibrium isotherm, kinetic and thermodynamic studies were conducted to assess the sorption behaviors.

2. Materials and methods

2.1. Reagents

Europium nitrate pentahydrate ($Eu(NO_3)_3 \bullet 5H_2O$) was purchased from Sigma-Aldrich Corp. (St. Louis, MO, USA). Cerium(IV) sulfate tetrahydrate ($Ce(SO_4)_2 \bullet 4H_2O$), dipotassium hydrogen phosphate (K_2HPO_4), ammonia solution and nitric acid were obtained from Merck. The stock solution of Eu(III) (1000 mg L^{-1}) was prepared by dissolving 2.82 g of $Eu(NO_3)_3 \bullet 5H_2O$ in 1000 mL deionized water. Test solutions of the chosen concentrations were prepared by diluting the stock solution in appropriate volumes. Nitric acid and ammonia solution were used for pH adjustments.

2.2. Preparation of cerium phosphate

The precipitation of amorphous cerium phosphate was reported by Hanna et al. [21]. According to this procedure, the stoichiometric amount of $Ce(SO_4)_2 \bullet 4H_2O$ and K_2HPO_4 was dissolved in deionized water and equimolar (0.012 mol L^{-1}) solutions of $Ce(SO_4)_2 \bullet 4H_2O$ and K_2HPO_4 were prepared separately. K_2HPO_4 solution was added to $Ce(SO_4)_2 \bullet 4H_2O$ solution dropwise with continuous stirring until the final pH of the solution was 2. The mixture obtained was stirred for 1 h more and kept 24 h at ambient temperature for aging. The yellow-colored precipitate was washed with deionized water to obtain a constant pH value. The formed gel was separated by centrifuge and dried at 60 ^{o}C.

2.3. Identification and characterization

Cerium phosphate powders were identified and characterized by X-ray Diffraction (XRD), scanning electron microscope (SEM), Fourier transform infrared (FTIR), and thermal analyses (TGA-DSC). XRD pattern

was recorded by Philips X'Pert Pro diffractometer (Philips Research Laboratories, Eindhoven, Netherlands). FTIR data (400-4000 cm^{-1}) were acquired by Perkin Elmer Spectrum Two model FTIR-ATR spectrometer (PerkinElmer, Inc. Waltham, MA USA). SEM images were collected using the Thermo Scientific Apreo S model scanning electron microscope (Thermo Fisher Scientific Inc., Waltham, MA, USA). TGA-DSC data were obtained by TA Instruments SDT Q600 up to 1000 ^{o}C with a heating rate of 10 ^{o}C min^{-1} (TA Instruments SDT Q600: TA Instruments, New Castle, DE, USA).

2.4. Statistical design of experiments

Response surface methodology (RSM) is a useful tool to evaluate the interactions of process variables [22]. RSM is composed of statistical and mathematical techniques to design experiments, establish numerical models, study the effects of variables, and search for the optimum combinations of factors. In experimental design methodology, variables vary from one experiment to the next simultaneously. As the variables may affect each other, the value of one variable can depend on the value of other variables [23].

Three-level designs have been suggested by Box and Behnken (1960) for fitting the response surfaces. In these designs, 2^k factorials are combined with incomplete block designs. The resulting designs are composed of a reduced number of required runs which make them efficient [24].

To investigate the effect of initial pH (X_1), contact time (X_2), and sorbent amount (X_3) on Eu(III) sorption, a three-level BBD has been used. According to BBD, a total of 15 runs with three replicates at center points were carried out. Statistical analyses were performed by Design Expert 12 software (Stat-Ease, Inc., Minneapolis, MN, USA). The effect of variables on Eu(III) sorption was investigated by batch method. The contact between sorbent and Eu(III) ions in solution was provided in a temperature-controlled shaker at 150 rpm by adding 0.05 g sorbent in 30 mL of liquid phase. When the sorption equilibrium was achieved, samples were filtered and Eu(III) concentrations were determined by ICP-OES.

Sorption capacity (Q) was calculated using Eq. (1):

$$Q = (C_o - C_e) \times \frac{V}{m} \ (\text{mg g}^{-1}) \tag{1}$$

Distribution coefficient (K_D) is defined as the ratio of metal concentration in the sorbent phase to solution-phase [25] and it is determined by Eq. (2):

$$K_D = \frac{C_0 - C_e}{C_e} \times \frac{V}{m} \ (\text{mL g}^{-1}) \tag{2}$$

In Eqs. (1) and (2), C_o and C_e are the initial and equilibrium concentrations of Eu(III) ion in solution (mg L^{-1}), V is the volume (mL) and m is the mass of the sorbent (g).

The ranges and levels of the variables (low, center, high) are presented in Table 1.

Table 1. Range and levels of process variables.

Variable		− 1	0	+ 1
Initial pH	X_1	2	4	6
Contact time (min)	X_2	60	120	180
Sorbent amount (g)	X_3	0.05	0.10	0.15

The general model equation including linear and quadratic terms for the estimation of optimum response is as follows:

$$y_i = b_0 + b_i X_i + b_{ii} X_{ii}^2 + b_{ij} X_i X_j \tag{3}$$

In Eq. (2), b_o denotes the intercept. b_i, b_{ii} and b_{ij} signify linear effects, quadratic effects and dual effects, respectively. The second-order polynomial equation related to the model can be written as follows:

$$y = b_0 + b_1 X_1 + b_2 X_2 + b_3 X_3 + b_{11} X_1^2 + b_{22} X_2^2 + b_{33} X_3^2 + b_{12} X_1 X_2 + b_{13} X_1 X_3 + b_{23} X_2 X_3 \tag{4}$$

2.5. Isotherm, kinetic and thermodynamic studies

2.5.1. Isotherm studies
30 mL of Eu(III) solutions at varying concentrations (25–400 mg L^{-1}) were separately prepared. After adjusting the pH of the solution to 4, 0.05 g cerium phosphate was added to each solution. The solid/liquid contact was carried out in a temperature-controlled shaker at 298 ± 1 K for 120 min.

2.5.2. Kinetic studies
Kinetic experiments were conducted between 15 and 360 min of contact time. 30 mL of 100 mg L^{-1} Eu(III) solutions were separately contacted with 0.05 g sorbent at pH 4. Kinetic models were applied to test the experimental data.

2.5.3. Thermodynamic studies
Experiments were carried out at 303, 313, 323, and 333 K for the determination of thermodynamic parameters such as enthalpy change (ΔH^o), entropy change (ΔS^o) and Gibbs free energy change (ΔG^o). For each temperature, 30 mL of 100 mg L^{-1} Eu(III) solution was shaken with 0.05 g of sorbent at pH 4 for 120 min.

For all experiments, initial and equilibrium concentration of Eu(III) ions were measured by ICP-OES. Eu(III) sorption capacity (Q) and distribution coefficient values (K$_D$) were calculated according to Eqs. (1) and (2), respectively.

3. Results and discussion

3.1. Characterization studies
XRD pattern of cerium phosphate is depicted in Figure 1a. It is seen that cerium phosphate has an amorphous structure. Figure 1b represents the IR spectrum of the cerium phosphate powders. The broad peak at 3196 cm^{-1} is assigned to –OH stretching vibrations and the peak at 1633 cm^{-1} is attributed to –OH bending vibrations of water molecule [26]. The bands around 992 cm^{-1} and 513 cm^{-1} correspond to P–O stretching and O–P–O bending mode of vibration, respectively [21].

TGA-DSC thermogram of cerium phosphate is demonstrated in Figure 1c. The thermogram was taken between 10 ^{o}C and 1000 ^{o}C at a uniform heating rate of 10 ^{o}C min^{-1}. The TGA curve shows a continuous decrease in the mass as a function of temperature. There are two weight loss regions. The weight loss between 25 ^{o}C and 310 ^{o}C, is mainly from the dehydration of physisorbed water molecules. Condensation of POH groups occurs from 310 ^{o}C to 1000 ^{o}C. The total weight loss is about 17.31%. In the DSC curve, the endothermic peak around 75 ^{o}C is attributed to the dehydration of water. The sharp exothermic peak at 620.33 ^{o}C is due to the crystallization of cerium polyphosphate. SEM image of cerium phosphate powders is given in Figure 1d.
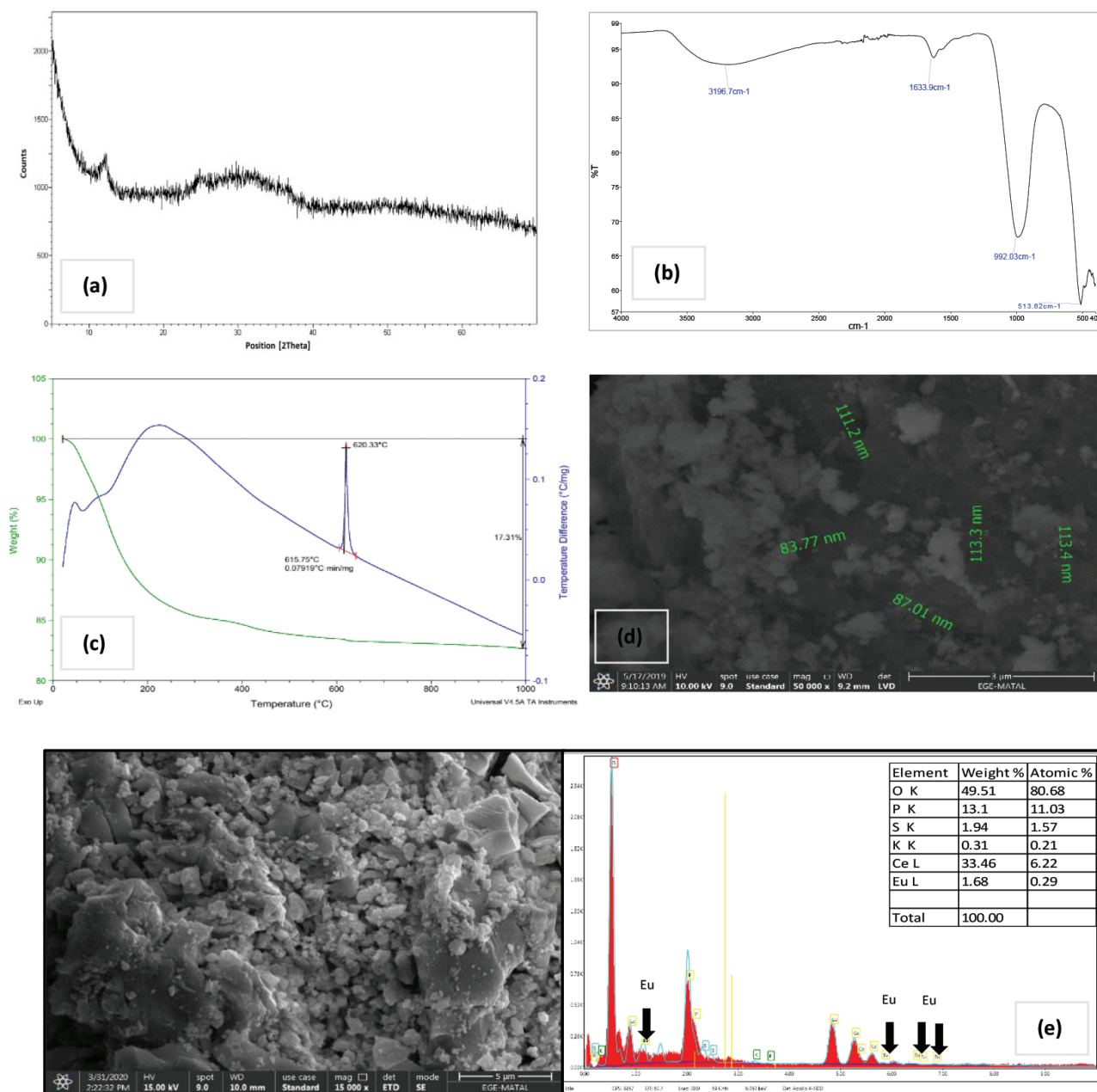
Figure 1. Characterization studies; a) XRD pattern, b) IR spectrum, c) TGA-DSC curve, d) SEM image before Eu(III) sorption, e) SEM image & EDX data after Eu(III) sorption.

Particles tend to form aggregates. Smaller particles with an approximate size of 80 to 120 nm were detected. SEM image and EDX data after Eu(III) sorption are presented in Figure 1e. There is no significant change in the SEM image after sorption. Particle size distribution is not homogeneous and aggregates can be seen. The presence of Eu(III) on the sorbent surface was confirmed by EDX data. The weight percentage of elements on the surface was also provided in Figure 1e.

3.2. Statistical analysis

BBD utilized in this study consists of 12 factorial and 3 replicate points. Experimental variables in coded and actual forms along with the response are presented in Table 2.

Table 2. Box-Behnken model for Eu(III) sorption onto cerium phosphate.

No	Initial pH	Contact time (min)	Sorbent amount (g)	Experimental Eu(III) capacity (mg g^{-1})	Predicted Eu(III) capacity (mg g^{-1})
1	- 1(2)	- 1(60)	0(0.10)	7.39	6.06
2	1(6)	- 1(60)	0(0.10)	15.55	18.46
3	- 1(2)	1(180)	0(0.10)	9.09	6.18
4	1(6)	1(180)	0(0.10)	23.05	24.39
5	- 1(2)	0(120)	- 1(0.05)	9.59	11.42
6	1(6)	0(120)	- 1(0.05)	41.87	39.44
7	- 1(2)	0(120)	1(0.15)	6.15	8.57
8	1(6)	0(120)	1(0.15)	12.98	11.16
9	0(4)	- 1(60)	- 1(0.05)	25.37	24.88
10	0(4)	1(180)	- 1(0.05)	27.19	28.28
11	0(4)	- 1(60)	1(0.15)	10.77	9.69
12	0(4)	1(180)	1(0.15)	11.85	12.34
13	0(4)	0(120)	0(0.10)	15.80	15.82
14	0(4)	0(120)	0(0.10)	15.66	15.82
15	0(4)	0(120)	0(0.10)	16.02	15.82

A second-order polynomial equation was used to express the relationship between independent variables and the response. The regression coefficients of parameters were determined and data were fitted to a second-order polynomial equation as given by Eq. (5):

$$y = 15.82 + 7.65nX_1 + 1.51X_2 - 7.78X_3 - 1.60X_1^2 - 0.45X_2^2 + 3.42X_3^2 + 1.45X_1X_2 - 6.36X_1X_3 - 0.19X_2X_3 \quad (5)$$

The statistical significance of the model is checked by ANOVA [27]. Table 3 represents the ANOVA results, coefficients, and P values. In Table 3, the model F value of 15.93 suggests that the proposed model is significant. The correlation coefficient (R^2) was found to be 0.97. It means that predicted capacity values are in good agreement with the experimental ones.

The smallest level of importance leading to rejection of the null hypothesis is described as the P-value. When P $<$ 0.05, the main effect and dual effects are regarded as statistically significant [28]. The main effect of initial pH ($P = 7.0 \times 10^{-4}$), the main effect of sorbent amount ($P = 6.0 \times 10^{-4}$), and dual effect of initial pH and sorbent amount ($P = 7.0 \times 10^{-3}$) were determined to be significant.

The positive value of coefficient belonging to pH ($X_1 = 7.65$) points out that pH has a positive effect on the sorption of Eu(III). It means that the uptake of Eu(III) increases as pH increases. The sorbent surface is mostly protonated at lower pHs. Eu(III) ions in solution compete with H^+ ions for the active surface sites. As the pH increases, the number of H^+ ions in the solution decreases, and the sorption of Eu(III) becomes more

Table 3. ANOVA, coefficients and P values for Eu(III) sorption onto cerium phosphate

ANOVA.						
	df	Sum of squares	Mean square	F value	Probability F	R^2
Regression	9	1199.432	133.270	15.927	0.004	0.97
Residuals	5	41.839	8.368			
Total	14	1241.271				
	Coefficients	P values				
Intercept	15.82	0.0002				
X_1	7.65	0.0007				
X_2	1.51	0.1992				
X_3	$-$ 7.78	0.0006				
X_1X_1	$-$ 1.60	0.3360				
X_2X_2	$-$ 0.45	0.7751				
X_3X_3	3.42	0.0720				
X_1X_2	1.45	0.3612				
X_1X_3	$-$ 6.36	0.0070				
X_2X_3	$-$ 0.19	0.9020				

favorable [29]. It is seen from Figure 2a that the sorption capacity of Eu(III) increases in the pH range of $2-6$. Maximum Eu(III) uptake is 21.87 mg g^{-1} at pH 6. Contact time ($X_2 = 1.51$) has a positive effect on sorption. Eu(III) sorption capacity slightly increases from 13.85 to 16.88 mg g^{-1} (Figure 2b).
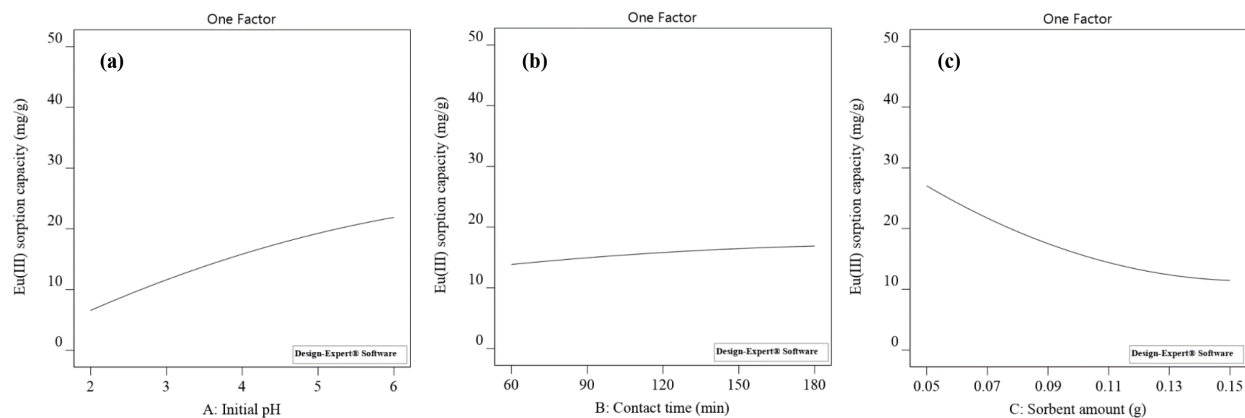
Figure 2. Main effects on Eu(III) sorption capacity; a) effect of initial pH, b) effect of contact time, c) effect of sorbent amount.

However, the coefficient of sorbent amount ($X_3 = - 7.78$) has a negative value. This implies that the sorption capacity of Eu(III) decreases with the increasing sorbent amount. Eu(III) uptake decreased from 27.03 to 11.46 mg g^{-1} with the increase in sorbent amount from 0.05 to 0.15 g (Figure 2c).

3.3. 3D Response surface plots

The relation between the dual effects of independent variables and Eu(III) sorption capacity (Q) was given in 3D surface plots (Figure 3). Figure 3a displays the change in Q values depending on initial pH (X_1) and contact time (X_2). Maximum Q was found to be 24.39 mg g^{-1} in 180 min, at initial pH 6 by holding the sorbent amount at 0.10 g.
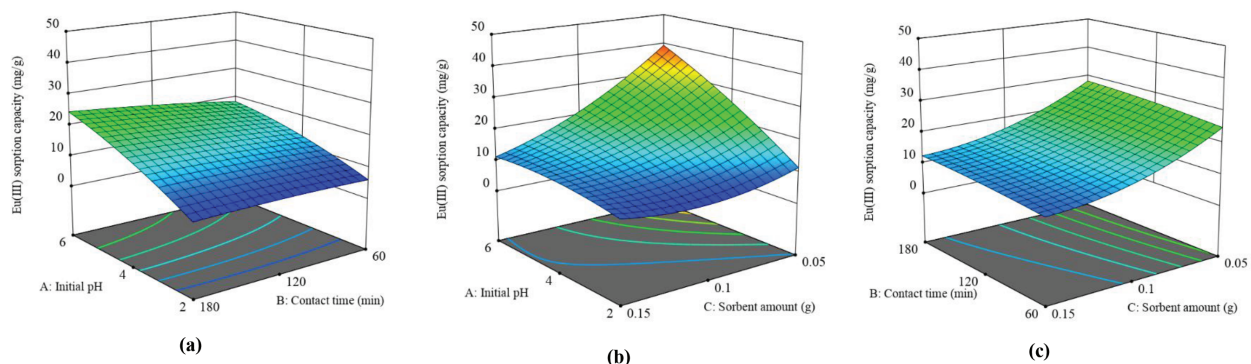

Figure 3. Response surface plots for dual effects; a) initial pH and contact time, b) initial pH and sorbent amount, c) contact time and sorbent amount.

Figure 3b shows the dual effect of initial pH (X_1) and sorbent amount (X_3). Maximum Q was 39.44 mg g^{-1} at initial pH 6 and sorbent amount of 0.05 g. The dual effect of contact time (X_2) and sorbent amount (X_3) at the initial pH 4 is shown in Figure 3c. It is inferred from Figure 3c that Q value gradually increases with the increase in contact time from 60 to 180 min. However, a significant decrease can be seen on the Q values by the increase in sorbent amount in the range of 0.05–0.15 g. Maximum Q was determined to be 28.28 mg g^{-1} in 180 min with 0.05 g sorbent.

3.4. Equilibrium isotherm, kinetic and thermodynamic studies

3.4.1. Isotherm studies

The effect of initial Eu(III) concentration on sorption was determined between 25–400 mg L^{-1}. Figure 4 demonstrates the relation between Q, K$_D$, and Eu(III) ion concentration at equilibrium. Eu(III) uptake increases from 12.17 to 29.47 mg g^{-1} with the increase in initial Eu(III) concentration from 25 to 200 mg L^{-1}. After this point, Eu(III) uptake reaches a plateau and remains almost constant. This behavior can be interpreted as the saturation of active sites on the sorbent. On the other hand, with the increase in initial Eu(III) concentration, K$_D$ values decrease since the number of ions in the solution increases more than the number of ions sorbed. The maximum K$_D$ value of 3632.2 mL g^{-1} was obtained when the initial Eu(III) concentration was 23.6 mg L^{-1}.

The sorption equilibrium data are expressed by sorption isotherms. Isotherms clarify the relationship between the metal concentration in the solution at equilibrium C_e and the mass of the metal sorbed per unit mass of sorbent q_e.

Langmuir's theory assumes that sorption occurs at specific homogeneous sites within the sorbent. Langmuir model in its linear form [30] is expressed as:

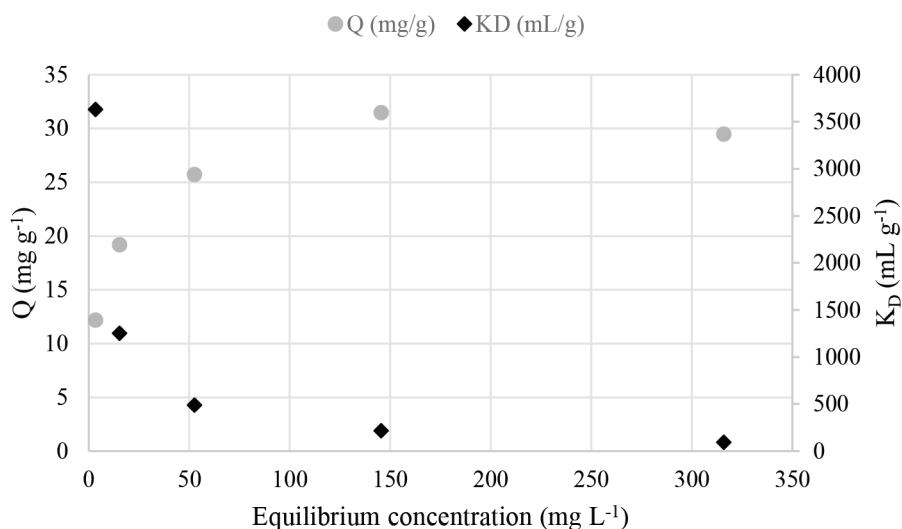$$\frac{C_e}{q_e} = \frac{1}{q_m b} + \frac{C_e}{q_m} \tag{6}$$

Figure 4. Sorption isotherm of Eu(III) onto cerium phosphate (initial pH: 4, temperature: 25 ^{o}C, contact time: 120 min).

where q_m is the maximum amount of the metal ion per unit weight of adsorbent to form a complete monolayer (mg g^{-1}), C_e is the equilibrium concentration of metal ion (mg L^{-1}) and b is a constant related to the sorption energy (L mg^{-1}). q_m and b values are calculated from the slope and intercept of the linear plot between C_e/q_e and C_e.

q_m, b, and correlation coefficient (R^2) values calculated from the isotherm are given in Table 4. q_m value was estimated to be 30.40 mg g^{-1}. An R^2 value of 0.99 indicates that the sorption data can be explained well by the Langmuir model.

Table 4. Isotherm model data for Eu(III) sorption onto cerium phosphate.

Isotherm model	Parameter	Value
Langmuir	q$_m$ (mg g^{-1})	30.40
	b (L mg^{-1})	0.18
	R^2	0.99
Freundlich	K$_f$	10.3
	n	4.83
	R^2	0.92
Dubinin–Radushkevich (D–R)	q$_m$ (mg g^{-1})	26.44
	E (kj mol^{-1})	0.50
	R^2	0.80

The separation factor (R_L) [31], which is based on the Langmuir model, can be represented as in Eq. (7):

$$R_L = \frac{1}{1 + bC_o} \tag{7}$$

where b is the Langmuir constant (L mg^{-1}) and C_o is the initial metal ion concentration (mg L^{-1}). If the value of R_L is between zero and one ($0 < R_L < 1$), the sorption is favorable. The calculated values of R_L

were plotted against initial Eu(III) concentration as shown in Figure 5. It can be deduced from Figure 5 that Eu(III) sorption is favorable for all concentrations under investigation.
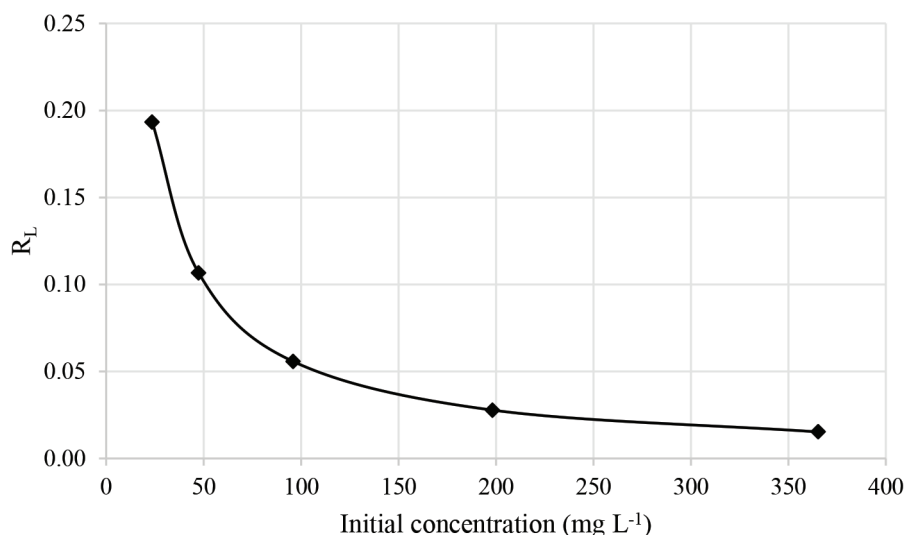

Figure 5. Dimensionless constant (R_L).

Freundlich adsorption isotherm [32] and its linear form can be described by Eq. (8) and Eq. (9), respectively:

$$q_e = K_f C_e^{\frac{1}{n}} \tag{8}$$

$$ln q_e = ln K_f + \frac{1}{n} ln C_e \tag{9}$$

where q_e is the equilibrium adsorption capacity (mg g^{-1}), C_e is the metal concentration at equilibrium, K_f and n are constants related to adsorption capacity and intensity, respectively. The values of n and K_f are shown in Table 4.

Dubinin-Radushkevich isotherm [33] is expressed as:

$$ln q_e = ln q_m - \beta \varepsilon^2 \tag{10}$$

ε is the Polanyi potential given by Eq. (11),

$$\varepsilon = RT ln \left(1 + \frac{1}{C_e} \right) \tag{11}$$

where β is a constant related to the mean free energy of adsorption (mol^2 J^2)$^{-1}$, q_e is the amount of solute adsorbed at equilibrium (mg g^{-1}), q_m is the theoretical saturation capacity (mg g^{-1}), R is the gas constant (R = 8.314 J mol^{-1} K^{-1}) and T is the temperature (K). The adsorption mean free energy E (kJ mol^{-1}) can be calculated as follows:

$$E = \frac{1}{\sqrt{2\beta}} \tag{12}$$

When the value of E is below 8 kJ mol^{-1}, the sorption process can be considered as physical sorption. However, the sorption process follows a chemical mechanism if the value of E is between 8–16 kJ mol^{-1}. The D-R isotherm constant and the value of E are summarized in Table 4. The adsorption mean energy value was obtained as 0.50 kJ mol^{-1}. This value indicates that physical sorption plays a dominant role in the sorption process.

The comparison of Eu(III) sorption capacity of amorphous cerium phosphate with some other sorbents reported in the literature is presented in Table 5.

Table 5. Comparison of Eu(III) sorption capacities of various sorbents.

Sorbent	Initial pH	Eu(III) Capacity (mg g^{-1})	Reference
Poly-acrylamide based Ce(IV) phosphate	2.0	91.2	[15]
Aluminum silicotitanate	4.0	45.9	[34]
Al^{3+} and Fe^{3+} modified titanium phosphates	6.0	39.0	[35]
Magnesia modified aluminum silicate	6.0	48.9	[6]
Al-substituted goethite	5.5	6.75	[5]
Cerium phosphate	6.0	42.14	Present study

As can be seen in Table 5, the obtained Eu(III) uptake value of cerium phosphate is comparable to the values reported in the literature. On the other hand, the uptake capacity of cerium phosphate can be enhanced by surface modification or doping of other elements.

3.4.2. Thermodynamic studies

The effect of temperature on Eu(III) sorption was examined at 303, 313, 323 and 333 K. Figure 6 illustrates the variation of Q and K$_D$ values as a function of temperature. Eu(III) uptake capacity slightly increases from 27.06 to 31.39 mg g^{-1} with the increase in temperature from 303 to 333 K. Similarly, a slight increase in K$_D$ values from 493.4 to 657.0 mL g^{-1} is observed in the same region.
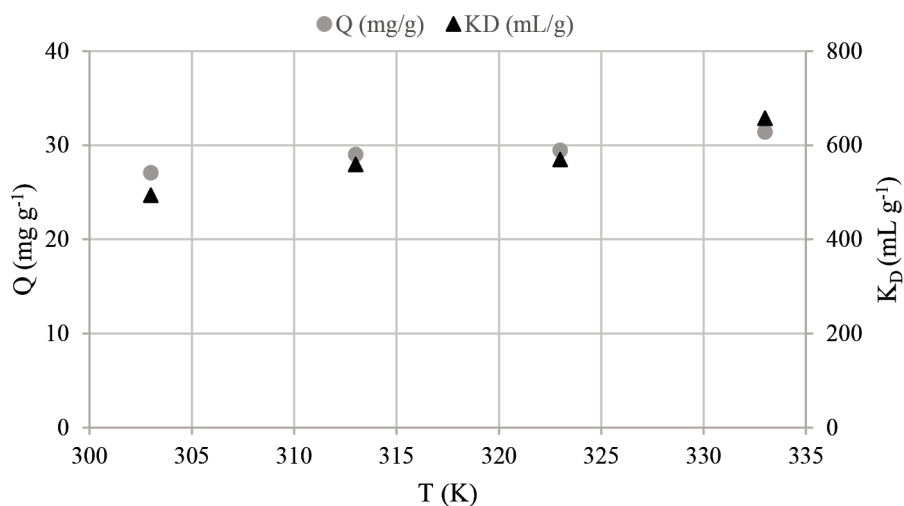

Figure 6. The effect of temperature for Eu(III) sorption onto cerium phosphate (initial pH: 4, initial concentration: 100 mg L^{-1}, sorbent amount: 0.05 g, contact time: 120 min).

Thermodynamic data provides information about the spontaneity of the sorption process. The values of ΔH^o, ΔS^o and ΔG^o were estimated using Eqs. (13), (14) and (15) [36]:

$$K_D = \frac{C_0 - C_e}{C_e} \times \frac{V}{m} \tag{13}$$

$$lnK_D = \frac{\Delta S^\circ}{R} - \frac{\Delta H^\circ}{RT} \tag{14}$$

$$\Delta G^\circ = \Delta H^\circ - T\Delta S^\circ \tag{15}$$

In the equations above, K_D is the thermodynamic equilibrium constant $(mL\ g^{-1})$, R is the universal gas constant $(8.314\ J\ mol^{-1}\ K^{-1})$, T is the temperature (K), V is the solution volume (mL) and m is the mass (g) of the sorbent. ΔH^o and ΔS^o were calculated from the slope and intercept of the plot between InK_D and $1/T$.

Thermodynamic parameters for Eu(III) sorption are given in Table 6. The negative values of ΔG^o obtained at 303, 313, 323, and 333 K point out the spontaneity of the Eu(III) sorption process.

Table 6. Thermodynamic parameters for Eu(III) sorption onto cerium phosphate.

Temperature (K)	ΔH^o (kJ mol^{-1})	ΔS^o (kJ mol^{-1} K^{-1})	ΔG^o (kJ mol^{-1})
303			− 16.89
313	7.35	0.08	− 17.69
323			− 18.49
333			− 19.29

The positive value of ΔH^o suggests that Eu(III) sorption is an endothermic process. The positive value of ΔS^o indicates the increase in randomness at the solid-liquid interface during sorption. In general, values of ΔG^o for physisorption are up to $-20\ kJ\ mol^{-1}$ while values between -80 and $-400\ kJ\ mol^{-1}$ indicate chemisorption mechanism [37]. The values of ΔG^o obtained in this study are within the ranges of physisorption mechanism.

3.4.3. Kinetic studies
Kinetic experiments were conducted between 5 and 360 min of contact time. The experimental kinetic data were evaluated using pseudo-first and pseudo-second-order kinetic models. Pseudo-first order model is expressed as:

$$\frac{dq_t}{dt} = k_1 (q_e - q_t) \tag{16}$$

The integrated form of the equation is:

$$ln(q_e - q_t) = lnq_e - k_1t \tag{17}$$

where k_1 is the first-order rate constant (min^{-1}), q_t and q_e are the amount of metal ion adsorbed $(mg\ g^{-1})$ at time t and equilibrium, respectively [38,39]. k_1 and q_e can be obtained from the slope and the intercept of the plot.

Pseudo-first order kinetic model is not suitable to describe the sorption of Eu(III), because the R^2 value is relatively low and the calculated q_e values are not per the experimental data.

The pseudo-second order model [40] is based on sorption capacity of sorbent and it is given by Eq. (18):

$$\frac{dq_t}{d_t} = k_2 (q_e - q_t) \tag{18}$$

where k_2 is the second order rate constant (g mg^{-1} min^{-1}). Integrated linear form of the equation is expressed as:

$$\frac{t}{q_t} = \frac{1}{k_2 q_e^2} + \frac{t}{q_e} \tag{19}$$

The kinetic plot of t/qt versus t for Eu(III) sorption is presented in Figure 7. q_e and k_2 can be calculated from the slope and the intercept of the plot.
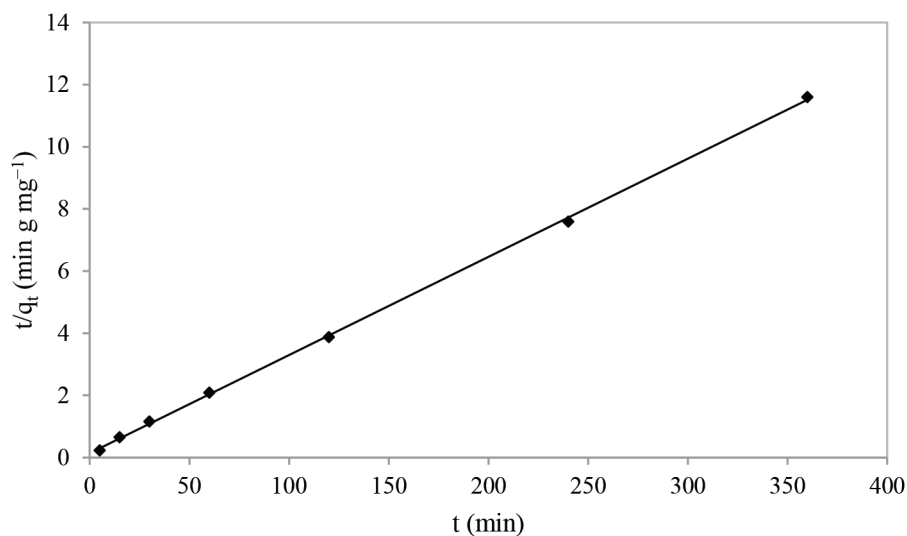

Figure 7. Pseudo-second order kinetic plot.

The pseudo-second-order model parameters q_e, k_2, and R^2 are provided in Table 7. Depending on R^2 values, the pseudo-second-order model suggests a better fit to experimental data.

Table 7. Kinetic model parameters for Eu(III) sorption.

Kinetic model	k_1 (min^{-1})	q_e (mg g^{-1})	R^2
Pseudo-first order	0.008	6.15	0.72
	k_2 (g mg min^{-1})	q_e (mg g^{-1})	R^2
Pseudo-second order	0.007	31.65	0.99

4. Conclusion

In this study, amorphous cerium phosphate was synthesized via a one-step method. Characterization studies were performed by XRD, SEM, FTIR, and thermal analyses. The relation between independent variables (initial pH, contact time, sorbent amount) and Eu(III) sorption capacity (Q) was investigated by Box-Behnken

design. The effect of initial pH and sorbent amount on Eu(III) sorption was found statistically significant by the evaluation of regression analyses and ANOVA. The correlation coefficient ($R^2 = 0.97$) points out the good agreement between actual and predicted Q values. The F value of the model was found to be 15.93 and it shows the significance of the model. 3D response surface plots were described to evaluate the dual effects of variables. The maximum Eu(III) sorption capacity of cerium phosphate was obtained as 42.14 mg g^{-1} at initial pH 6, contact time of 180 min, and sorbent amount of 0.05 g.

Langmuir model is the best to describe the sorption of Eu(III) and monolayer Eu(III) sorption capacity was found to be 30.40 mg g^{-1}. The positive value of ΔH^o expresses the endothermic character of sorption. A decrease in ΔG^o values with increasing temperature supports the assumption that the sorption process is spontaneous. Based on the value of R^2, the pseudo-second-order model was best to fit the kinetic data.

Overall results point out that amorphous cerium phosphate is an easily prepared sorbent capable of removing Eu(III) ions from a slightly acidic aqueous solution.

Acknowledgment

References

1. Rim KT, Koo KH, Park JS. Toxicological evaluations of rare earths and their health impacts to workers: a literature review. Safety and Health at Work 2013; 4 (1): 12-26. doi: 10.5491/SHAW.2013.4.1.12

2. Binnemans K, Jones PT, Blanpain B, Gerven TV, Yang YX et al. Recycling of rare earths: a critical review. Journal of Cleaner Production 2013; 51: 1-22. doi: 10.1016/j.jclepro.2012.12.037

3. Furuhashi Y, Honda R, Noguchi M, Hara-Yamamura H, Kobayashi S et al. Optimum conditions of pH, temperature and preculture for biosorption of europium by microalgae Acutodesmus acuminatus. Biochemical Engineering Journal 2019; 143: 58-64. doi: 10.1016/j.bej.2018.12.007

4. Hassan HS, Madcour WE, Elmaghraby EK. Removal of radioactive cesium and europium from aqueous solutions using activated Al_2O_3 prepared by solution combustion. Materials Chemistry and Physics 2019; 234: 55-66. doi: 10.1016/j.matchemphys.2019.05.081

5. Li M, Liu H, Chen T, Hayat T, Alharbi NS et al. Adsorption of europium on Al-substituted goethite. Journal of Molecular Liquids, 2017; 236: 445-451. doi: 10.1016/j.molliq.2017.04.046

6. Mansy MS, Hassan RS, Selim YT, Kenawy SH. Evaluation of synthetic aluminum silicate modified by magnesia for the removal of ^{137}Cs, ^{60}Co and $^{152+154}Eu$ from low-level radioactive waste. Applied Radiation and Isotopes 2017; 130: 198-205. doi: 10.1016/j.apradiso.2017.09.042

7. Hamza MF, Roux J-C, Guibal E. Uranium and europium sorption on amidoxime-functionalized magnetic chitosan micro-particles. Chemical Engineering Journal 2018; 344: 124-137. doi: 10.1016/j.cej.2018.03.029

8. Verma PK, Semenkova AS, Krupskaya VV, Zakusin SV, Mohapatra PK et al. Eu(III) sorption onto various montmorillonites: experiments and modeling. Applied Clay Science 2019; 175: 22-29. doi: 10.1016/j.clay.2019.03.001

9. Sofronov D, Krasnopyorova A, Efimova N, Oreshina A, Bryleva E et al. Extraction of radionuclides of cerium, europium, cobalt and strontium with Mn_3O_4, MnO_2, and MNOOH sorbents. Process Safety and Environmental Protection 2019; 125: 157-163. doi: 10.1016/j.psep.2019.03.013

10. Diniz V, Volesky B. Biosorption of La, Eu and Yb using Sargassum biomass. Water Research 2005; 39 (1): 239-247. doi: 10.1016/j.watres.2004.09.009

11. Apsara AP, Beena B. Ion exchange properties of synthesized cerium (IV) phosphate. Research Journal of Chemical and Environmental Sciences 2014; 2 (1): 18-23.

12. El-Kamash AM, El-Gammal B, El-Sayed AA. Preparation and evaluation of cerium(IV) tungstate powder as inorganic exchanger in sorption of cobalt and europium ions from aqueous solutions. Journal of Hazardous Materials 2007; 141: 719-728. doi: 10.1016/j.jhazmat.2006.07.041

13. Kapnisti MG, Noli FG, Papastergiadis ES, Pavlidou EG. Exploration of the parameters affecting the europium removal from aqueous solutions by novel synthesized titanium phosphates. Journal of Environmental Chemical Engineering 2018; 6: 3408-3417. doi: 10.1016/j.jece.2018.05.010

14. Garcia-Glez J, Trobajo C, Khainakov SA, Amghouz Z. α-Titanium phosphate intercalated with propylamine: an alternative pathway for efficient europium(III) uptake into layered tetravalent metal phosphates. Arabian Journal of Chemistry 2017; 10 (6): 885-894. doi: 10.1016/j.arabjc.2016.07.013

15. Metwally SS, El-Gammal B, Aly HF, Abo-El-Enein SA. Removal and separation of some radionuclides by poly-acrylamide based Ce(IV) phosphate from radioactive waste solutions. Separation Science and Technology 2011; 46: 1808-1821. doi: 10.1080/01496395.2011.572328

16. El-Gammal B, Shady SA. Chromatographic separation of sodium, cobalt and europium on the particles of zir-conium molybdate and zirconium silicate ion exchangers. Chemical Engineering Journal 2018; 344: 124-137. doi: 10.1016/j.colsurfa.2006.02.068

17. Verma S, Bamzai KK. Preparation of cerium orthophosphate nanosphere by coprecipitation route and its structural, thermal, optical, and electrical characterization. Journal of Nanoparticles 2014; 2014: 1-12. doi: 10.1155/2014/125360

18. Masui T, Hirai H, Imanaka N, Adachi G. Characterization and thermal behavior of amorphous cerium phosphate. Physica Status Solidi A 2003; 198 (2): 364-368. doi: 10.1002/pssa.200306623

19. Wenwei W, Yanjin F, Xuehang W, Sen L, Xiufu H et al. Preparation of nano-sized cerium and titanium pyrophos-phates via solid-state reaction at room temperature. Rare Metals 2009; 28 (1): 33-38. doi: 10.1007/s12598-009-0007-5

20. Nilchi A, Ghannadi Maragheh M, Khanchi AR. Properties, ion-exchange behavior, and analytical applications of cerium phosphate cation exchangers suitable for column use. Separation Science and Technology 1999; 34 (9): 1833-1843. doi: 10.1081/SS-100100741

21. Hanna AA, Mousa SM, Elkomy GM, Sherief MA. Synthesis and microstructure studies of nano-sized cerium phosphates. European Journal of Chemistry 2010; 1 (3): 211-215. doi: 10.5155/eurjchem.1.3.211-215.69

22. Box GEP, Draper NR. Empirical Model-Building and Response Surfaces. New York, NY, USA: Wiley, 1987.

23. Gunaraj V, Murugan N. Application of response surface methodologies for predicting weld base quality in sub-merged arc welding of pipes. Journal of Materials Processing Technology 1999; 88: 266-275.

24. Montgomery DC. Design and Analysis of Experiments. Hoboken, NJ, USA: John Wiley & Sons, 2001.

25. Sivaiah MV, Venkatesan KA, Krishna RM, Sasidhar P, Murthy GS. Ion exchange studies of europium on ura-nium antimonate. Colloids and Surfaces A: Physicochemical and Engineering Aspects 2004; 236: 147-157. doi: 10.1016/j.colsurfa.2004.02.006

26. Bo L, Liya S, Xiaozhen L, Shuihe Z, Yumei Z et al. Sol-gel synthesis of monazite-type cerous phosphate for fiber coating. Journal of Materials Science Letters 2001; 20: 1071-1075. doi: 10.1023/A:1010985130019

27. Mourabet M, El Rhilassi A, El Boujaady H, Bennani-Ziatni M, El Hamri R et al. Removal of fluoride from aqueous solution by adsorption on hydroxyapatite (HAp) using response surface methodology. Journal of Saudi Chemical Society 2015; 16 (6): 603-615. doi: 10.1016/j.jscs.2012.03.003

28. Carmona MER, Silva MAP, Leite SGF. Biosorption of chromium using factorial experimental design. Process Biochemistry 2005; 40: 779-788. doi: 10.1016/j.procbio.2004.02.024

29. İnan S, Altaş Y. Preparation of zirconium–manganese oxide/polyacrylonitrile (Zr–Mn oxide/PAN) composite spheres and the investigation of Sr(II) sorption by experimental design. Chemical Engineering Journal 2011; 168: 1263-1271. doi: 10.1016/j.cej.2011.02.038

30. Langmuir I. The adsorption of gases on plane surfaces of glass, mica and platinum. Journal of the American Chemical Society 1918; 40: 1361-1403.

31. Foo KY, Hameed BH. Insights into the modeling of adsorption isotherm systems. Chemical Engineering Journal 2010; 156: 2-10. doi: 10.1016/j.cej.2009.09.013

32. Freundlich HMF. Over the adsorption in solution. The Journal of Physical Chemistry 1906; 57: 385-471.

33. Dubinin LV, Zaverina MM, Radushkevich ED. Sorption and structure of active carbons I. Adsorption of organic vapors. Zhurnal Fizicheskoi Khimii 1947; 21: 1351-1362.

34. Borai EH, Attallah MF, Elgazzar AH, El-Tabl AS. Isotherm and kinetic sorption of some lanthanides and iron from aqueous solution by aluminum silicotitante exchanger. Particulate Science and Technology 2019; 37: 410-422. doi: 10.1080/02726351.2017.1385550

35. Misaelides P, Sarri S, Zamboulis D, Gallios G, Zhuravlev I et al. Separation of europium from aqueous solutions using Al^{3+}- and Fe^{3+}- doped zirconium and titanium phosphates. Journal of Radioanalytical and Nuclear Chemistry 2006; 268: 53-58. doi: 10.1007/s10967-006-0123-8

36. Nayak AK, Pal A. Green and efficient biosorptive removal of methylene blue by Abelmoschus esculentus seed: process optimization and multi-variate modeling. Journal of Environmental Management 2017; 200: 145-159. doi: 10.1016/j.jenvman.2017.05.045

37. Gerçel Ö, Özcan A, Özcan AS, Gerçel HF. Preparation of activated carbon from a renewable bioplant of Euphorbia rigida by H_2SO_4 activation and its adsorption behavior in aqueous solutions. Applied Surface Science 2007; 253: 4843-4852. doi: 10.1016/j.apsusc.2006.10.053

38. Lagergren S. About the theory of so-called adsorption of solution substances. Kungliga Svenska Vetenskapsakademiens Handlingar 1898; 24: 147-156.

39. Ho YS, Mckay G. Sorption of lead(II) ions on peat. Water Research 1999; 33: 578-584. doi: 10.1016/S0043-1354(98)00207-3

40. Mahajan G, Sud D. Kinetics and equilibrium studies of Cr(VI) metal ion remediation by Arachis hypogea shell: a green approach. Bioresource Technology 2011; 6: 3324-3338. doi: 10.15376/biores.6.3.3324-3338